UCRL 8354 Rev

UNIVERSITY OF CALIFORNIA

Radiation Laboratory

BERKELEY, CALIFORNIA

DISCLAIMER

UCRL-8354 Rev.

UNIVERSITY OF CALIFORNIA

Radiation Laboratory
Berkeley, California

Contract No. W-7405-eng-48

ANGULAR DISTRIBUTION OF PHOTOPIONS FROM HYDROGEN

Edward A. Knapp, Robert W. Kenney, and Victor Perez-Mendez

October 3, 1958

Printed for the U.S. Atomic Energy Commission

ANGULAR DISTRIBUTIONS OF PHOTOPIONS FROM HYDROGEN

Edward A. Knapp, Robert W. Kenney and Victor Perez-Mendez

Radiation Laboratory
University of California
Berkeley, California

October 3, 1958

ABSTRACT

An accurate measurement of the differential cross section for the photoproduction of positive pions from protons has been made at the Berkeley synchrotron for photon energies of 260 and 290 Mev. The mesons were produced in a thin-walled liquid-hydrogen target, and the meson-detection apparatus utilized the characteristic decay of the pion. The measurements were done in two steps, from 0° to 50° with equipment specifically designed to reduce a very high forward-angle positron background, and from 30° to 160° with equipment whose efficiency and solid angle could be accurately determined.

The abrupt flattening of the observed cross section in the region forward of 40° is due to "photoelectric ejection" of pions from the cloud surrounding the nucleon. The results are compared to the theory of photoproduction derived from the dispersion relations, and the agreement is satisfactory within the limitations of the theory.

ANGULAR DISTRIBUTION OF PHOTOPIONS FROM HYDROGEN

Edward A. Knapp, Robert W. Kenney, and Victor Perez-Mendez

Radiation Laboratory
University of California
Berkeley, California

October 3, 1958

INTRODUCTION

The photoproduction of positive pions from hydrogen is one of the fundamental reactions encountered in the study of pi-meson phenomena and as such has been investigated quite extensively wherever high-energy photon beams have been available.[1-10] Recently, however, with the advent of more refined theories describing the photopion interaction,[11,12] there has been a revival of interest in the measurement of the reaction, for the existing data are insufficient to confirm some of the finer details of these theories.

Very little experimental information has hitherto been available on the angular distribution of this reaction in the angular region from 0° to 40°, where it is more difficult to make accurate measurements owing to the high electron background present. Furthermore, the existing data over the remaining angular range were neither internally consistent between the various laboratories nor statistically accurate enough to enable a critical selection between the various forms of the theories to be made.

With this in mind, the measurement of the differential cross section was undertaken, with the dual aims of obtaining data in the region forward of 40° (c.m.) and of materially reducing the errors associated with the values of the cross section over the angular interval from 40° to 160°. Our measurements were made in two steps: from 0° to 50° (c.m.) with equipment specifically designed to reduce the background, and from 30° to 160° with more conventional apparatus, which allowed enough overlap for careful normalization.

Similar experiments on the forward-angle region have been done by Lazarus[13] at Stanford University and by Malmberg and Robinson[14] at the University of Illinois. These experiments (performed at different energies and by different techniques) show essentially the same behavior as the results reported here.

EXPERIMENTAL PROCEDURE

A. Electronics

In both the small-angle and large-angle regions the mesons were detected by identifying their π-μ decay by the use of a well-known delayed-coincidence techniques. A full description of the electronic apparatus used in this experiment has been reported elsewhere.[15] Figure 1 shows a block diagram of the electronics. Briefly, its operation is as follows: When the correct combination of coincidence and anticoincidence pulses is registered in the multiple coincidence-anticoincidence unit, a 6×10^{-8}-sec gate is formed by the gate generator. This gate is placed in delayed coincidence with pulses from the scintillator in which the pion stops, the delay being so adjusted that a pion which has come to rest in the stopping counter (and thus is of the correct energy) is registered in Coincidence 1 if it decays between 3×10^{-8} and 9×10^{-8} sec after coming to rest. It is also possible for accidental counts to occur in Coincidence 1 from two particles passing through separated by between 3 and 9×10^{-8} sec., or from μ-e decays in this interval. Since these events are not strongly dependent on the delay time of the gate, they may be measured by making a coincidence with an identical gate delayed several pion half-lives from the pulse of the stopping pion. Coincidence 2 delayed by 12×10^{-8} sec serves this function.

B. Counter Telescopes and Experimental Arrangements

The channel and telescope used in the small-angle measurements are shown in Fig. 2. The 340-Mev bremsstrahlung beam from the Berkeley synchrotron was incident on a liquid-hydrogen container; the mesons produced were deflected by a magnetic channel and were detected by the counter telescope shown at the end of the channel. The target had thin walls made of Mylar, a material which, by virtue of its low atomic number, does not produce a large background of electron pairs.

The entrance and exit windows of the target vacuum jacket were sufficiently isolated from the target volume so that they made no appreciable contribution to the background. A sweeping magnet was provided between the entrance window and the target to remove any electrons or positrons from the incoming beam.

Positive particles, deflected by the magnetic field, were incident upon a lead filter placed as shown in Fig. 2. The positrons incident on this lead initiate showers with quite high probability and thus are removed from the beam, while the pions undergo some Coulomb scattering but are attenuated much less than the positrons. The thickness of this lead was chosen to minimize the positron flux at the telescope while keeping the loss of mesons due to multiple Coulomb scattering as small as possible. For the 260-Mev photons, 1.5 cm of lead was used, as shown in Fig. 2, presenting 2.75 radiation lengths to the positrons. For the 290-Mev photons, 2.5 cm was used.

The counter telescope required a triple coincidence (1, 3, and 4) to trigger the gate generator. Counters 2 and 6 were placed in anticoincidence. Counter No. 2 is a Cherenkov counter viewed by two RCA-6810 photomultiplier tubes whose outputs were added. The sensitive area was made of plexiglas, which has an index of refraction of 1.49, and is 2 in. thick. Any particle passing through the counter with a value of β greater than 0.67 produces a pulse, and hence a coincidence will not be recorded. Mesons entering this counter have $\beta = 0.64$ and thus do not make anticoincidence pulses. Positrons and electrons will produce pulses and thus will not trigger the gate. Counter 6 rejects any particle which passes through the entire telescope. All of these scintillators utilized 30-in. light pipes to remove the photomultiplier tubes from the high magnetic-field region.

The energy of the meson is determined by its range, which is set by changing the amount of copper absorber placed before the telescope. The ΔE_{π} accepted by the telescope is sufficiently narrow so that the magnetic selection had no effect on the energy band accepted by the counter telescope.

The arrangement used for the wide-angle measurements is shown in Fig. 3. The mesons are again produced in a liquid-hydrogen target, which in this case is a cylinder 3 in. in diameter. The telescope consists of three scintillators to trigger the gate generator, a stopping scintillator, and a large scintillator in anticoincidence to reject all particles passing through the entire telescope. The solid angle subtended by this telescope is determined by the area of the front scintillator. The following counters are successively larger in such a way that multiple-coulomb scattering of the mesons in coming to rest may be neglected or easily estimated. This removes one energy-dependent correction from the analysis of the data. The laboratory energy

of the meson is determined by the amount of copper absorber placed between the second and third scintillators. The whole counter-telescope assembly was placed on a cart which was pivoted about the center of the target volume, and angles could be set of 0.1° accuracy.

C. Monitoring

The primary monitor for the bremsstrahlung beam in this experiment was a thick-walled ion chamber identical to one calibrated versus the total energy content of the beam at Cornell University.[16] This chamber has 1-in.-thick copper walls, making it preferentially sensitive to the high-energy portion of the bremsstrahlung spectrum and insensitive to low-energy electrons in the beam.

The calibrated efficiency of this chamber is 3.79×10^{12} Mev per microcoulomb of charge collected; this number is then the value used in computing the absolute cross sections given in this paper.

COUNTER-TELESCOPE CALIBRATION

The efficiency of the π-μ counter telescope used in the wide-angle measurements was determined experimentally in a pi-meson beam at the Berkeley 184-inch cyclotron. The efficiency of this counter may be separated into two factors: one which arises from the loss of mesons that decay outside the gate pulse (electronic efficiency), the other from the loss of mesons by nuclear absorption and scattering as they come to rest in the stopping scintillator. At the cyclotron, both the electronic efficiency and the total efficiency were measured. When the absorption loss was calculated from previous experimental data and combined with the electronic efficiency, the two methods of calibration agreed very well, as shown in Fig. 4.

In order to determine the total efficiency experimentally, which is the product of the two factors above, first the various constituents of the pi beam were determined. This was done by measuring a range curve. Since the μ-meson and electron contamination in the beam have longer ranges than the pions, it is possible to determine the fraction of pions in the original beam.

Then the π-μ counter was placed in the beam, and the number of mesons counted by π-μ decay were determined. Because the ΔE_π of the telescope was somewhat smaller than the ΔE_π of the beam, the telescope counting rate was determined for several values of the mean pion-acceptance energy within the energy band of the beam, and the total number counted was determined by an appropriate summation. The ratio of the pions counted by π-μ decay to the number incident determines the efficiency. This procedure was undertaken at pion energies of 72, 87.5, and 115 Mev.

The efficiency may also be determined in an independent manner, which serves as a check on the method described above. It is possible to determine the electronic efficiency separately, and then compute the total efficiency from this. In order to accomplish this, the telescope absorber was adjusted so that only pions stopped in the stopping scintillator. Then the gate was centered on the pulse of the stopping pion. The ratio of delayed counts to undelayed counts gives directly the efficiency due to electronics. The loss due to nuclear absorption was calculated from the known absorption cross sections in various elements,[17] and the number of pions lost by multiple-coulomb scattering and diffraction scattering was estimated. The total efficiency was obtained in an independent way by combining the electronic efficiency with the other calculated losses.

Figure 4 shows the results of these measurements. The solid line is the efficiency determined by the calculation of the absorption loss coupled with the electronic efficiency. The experimental points represent the efficiency directly determined from the cyclotron calibration described above. The errors quoted on these points represent estimates on possible systematic errors and do not represent statistical counting errors which were much smaller.

CALCULATION OF CROSS SECTION FROM MEASURED COUNTING RATES

A general expression relating the observed counting rate in the wide-angle telescope to the differential cross section may be written

$$\frac{d\sigma}{d\Omega^*} = Y \cdot \frac{d\Omega}{d\Omega^*} \cdot \frac{1}{\Omega} \cdot \frac{1}{t} \cdot \frac{1}{\epsilon} \cdot \frac{A}{n} \cdot \frac{k}{h} \left(\frac{dE_\pi}{dk}\right)_{\theta_{lab}} \cdot \frac{1}{\Delta E_\pi} . \qquad (1)$$

Here $\frac{d\sigma}{d\Omega^*}$ is the differential cross section in the center-of-mass system; Y is the number of counts per microcoulomb charge integrated from the "Cornell" ionization chamber; $\frac{d\Omega}{d\Omega^*}$ is the lab. to c.m. solid-angle transformation; Ω is the solid angle subtended by the telescope in the laboratory system; t is the thickness of the liquid-hydrogen target in hydrogen nuclei per cm^2; ϵ is the efficiency of the counter telescope; A is $\int_0^{340} kN(k)dk$ for for the bremsstrahlung spectrum, normalized to $\left[kN(k)\right]_{k=0}=1$, measured in Mev; n is the ratio of the total energy in the beam to the integrated charge from the ionization chamber in Mev per microcoulomb; k is the mean energy of the photon inducing the reaction; h equals kN(k) for the normalized bremsstrahlung spectrum at k; $\left(\frac{dE_\pi}{dk}\right)_{\theta_{lab}}$ is the change in pion energy with photon energy evaluated at a fixed laboratory angle; and ΔE_π is the pion energy interval accepted by the telescope.

The kinematics of this reaction have been calculated on the Illiac digital computer by Malmberg and Koester,[18] and these tables have been used to determine the quantities $d\sigma/d\Omega^*$ and E_π as a function of the angle for a given photon energy. Here $(dE_\pi/dk)_{\theta_{lab}}$ was obtained by numerical differentiation of these tables. The value of N is obtained from a calibration of the ionization chamber undertaken at Cornell University, and is taken to be 3.79×10^{12} Mev/microcoulomb at k_{max} = 340 Mev. The pion-energy interval to which the counter was sensitive was computed by determining the range of energy covered by pions that would stop in the stopping scintillator, with a small correction applied for edge effects. This quantity is a function of the

mean energy of pions stopped in the scintillator and thus varies with angle for a given photon energy. The efficiency, ϵ, of the counter used in the large pion-angle investigation is determined from the calibration data taken at the cyclotron, with an additional correction applied for meson decay in flight.

In the small-angle studies, only a relative measurement of $\frac{d\sigma}{d\Omega^*}$ was required, so that only the parts of the above general expression which depend on the angle need be evaluated. In this case, we have

$$d\sigma/d\Omega^* \propto Y \cdot d\Omega/d\Omega^* \cdot 1/\epsilon' \cdot (dE_\pi/dk) \cdot 1/\Delta E_\pi , \qquad (2)$$

where in this expression ϵ' need not be absolute but need only reflect the variation of efficiency with pion energy. This may be computed from the known pion absorption cross sections. The other quantities are computed as before.

The error associated with the relative angular distributions is taken to be that introduced by the counting statistics only. Systematic errors that would alter the distribution might occur in the computation of ΔE_π and ϵ', but it is felt these quantities are known well enough to be certain that their contribution to the error is negligible. However, more serious systematic errors are possible in the evaluation of the absolute value of these points, the most serious of which is the calibration of the photon-beam ionization chamber. Estimates of the uncertainties in the absolute determinations gives an error for the total cross section of about 7%.

Table I gives the data in terms of the differential cross section in the center-of-mass system.

The small-angle measurements have been normalized by a least-squares procedure to the large-angle data in the angular region of overlap. In no case were these points separated by more than one standard deviation after normalization and the normalization error has been propagated to the small-angle points.

Table I

Angular distribution of photopions from hydrogen

260 Mev		290 Mev	
θ^*	$\frac{d\sigma}{d\Omega^*}$ (μb/sterad)	θ^*	$\frac{d\sigma}{d\Omega^*}$ (μb/sterad)
0	6.62 ± 0.65	0	6.90 ± 0.58
10	6.68 ± 1.13	10	7.16 ± 1.07
20	6.46 ± 0.76	20	7.62 ± 0.73
25	6.55 ± 0.87	30	6.96 ± 0.48
30	6.49 ± 0.51	40	9.23 ± 0.58
40	7.92 ± 0.49	50	11.90 ± 0.43
53	10.60 ± 0.50	70	15.90 ± 0.51
70	15.35 ± 0.39	90	19.86 ± 0.46
90	17.59 ± 0.47	115	19.50 ± 0.54
115	17.88 ± 0.37	140	16.72 ± 0.40
140	17.60 ± 0.34	160	13.76 ± 0.59
160	16.47 ± 0.38		
σ_{total} = 185 ± 13.5 microbarns		σ_{total} = 199 ± 14 microbarns	

DISCUSSION

The data from Table I are shown in Figs. 5 and 6, along with the data obtained previously at the California Institute of Technology by magnet[6] and counter telescope[7] techniques, and with the data compilation of Bernardini et al.[8] Examination of these points shows that while all previous sets of data have the same gross features, namely the peaking around 90° c.m., and the asymmetric forward-to-backward ratio, there are inconsistencies in the specific shapes of the curves which appear to be outside that ascribed to the statistical errors associated with the measurements. This inconsistency is most apparent at 290 Mev, where the counter-telescope data from the California Institute of Technology is larger than the magnet data in the forward direction, and smaller in the backward direction. The same effect will be noted in the 260-Mev data, although to a lesser degree. The measurements reported here indicate that the behavior of the differential cross section is essentially that of the magnet group forward from 90° and that of the counter telescope group at angles greater than 90°.

In the angular region forward from 40° c.m., the measured differential cross section at both 260 and 290 Mev is constant within the statistical accuracy of our measurements. Moravcsik[19] has pointed out that this behavior arises from the existence in the dispersion-relations theory for photoproduction[12] of a term with the following form:

$$\frac{(\vec{\epsilon}\cdot\vec{q})\,\vec{\sigma}\cdot(\vec{k}-\vec{q})}{q_0 k - \vec{q}\cdot\vec{k}}\,, \qquad (3)$$

where $\vec{k}$ and $\vec{\epsilon}$ are the photon momentum and polarization, $\vec{q}$ and q_0 are the momentum and energy of the meson, and $\vec{\sigma}$ is the nucleon spin. The denominator of this expression may also be written as $q_0 k(1-\beta\cos\theta^*)$, where θ^* is the pion emission angle in the center-of-mass system and β is the meson velocity. Since β is quite large at these energies, this term can become quite important in the forward angular region where $\cos\theta^*$ is close to 1. This term in the matrix element corresponds to the direct ejection of a virtual meson from the cloud surrounding the nucleon. The remaining terms in the photoproduction amplitude correspond to absorption of the photon by the nuclear core and involve positive powers of $\cos\theta$.

To include all the terms in the data analysis, Moravcsik has suggested fitting the observed angular distribution with an expression of the form:

$$\frac{d\sigma}{d\Omega^*} = \sum_{n=0}^{4} \frac{A_n \cos^n \theta^*}{(1-\beta \cos \theta^*)^2} \quad , \tag{4}$$

where the A_n are to be determined by a least-squares fit to the data. This expansion has been performed for our data, and the resulting curves are shown in Figs. 7 and 8. The values of the A_n obtained are given in Table II. These coefficients are not simply related to quantities of physical interest. However, the curve they represent gives a true indication of the shape of the angular distribution and may be used to compare experimental distributions with theoretical predictions.

Thus, in a recent paper, Taylor, Moravcsik and Uretsky[20] have used the analytical form for the differential cross section given in Eq. (4) to calculate the pion-nucleon coupling constant by the following extrapolation procedure. These authors show that by making an analytic continuation of the functional form for $\frac{d\sigma}{d\Omega}_*$ to an imaginary angle θ_0 where $\cos \theta_0 = 1/\beta$, they can then evaluate the residue at the pole at that angle. Then the coupling constant f^2 is determined by their theory from the measured differential cross sections alone, without any assumptions about charge independence.

The values obtained for f^2, using the values of the coefficients A_n given in Table II are:

$$f^2 = 0.131 \pm 0.037 \quad \text{for} \quad E_\gamma = 260 \text{ Mev}$$

$$f^2 = 0.016 \pm 0.031 \quad \text{for} \quad E_\gamma = 290 \text{ Mev}.$$

The errors in the values of f^2 obtained by this method are quite large because the numerical accuracy of the extrapolating procedure depends heavily on the experimental errors in the small-angle measurements.

A theoretical formula based on dispersion theory[12] has recently been evaluated by Uretsky et al.[21] using various assumptions about the small pion-nucleon phase shifts that enter the calculations but which are not known well experimentally.[22] In the initial calculations made by Uretsky, the P-wave

Table II

Values of A_n at 260 and 290 Mev

E_γ (Mev)	A_0	A_1	A_2	A_3	A_6
260	17.467	-31.475	9.907	6.603	-2.118
290	19.524	-36.867	9.479	16.272	-8.132

pion-nucleon scattering phase shifts were computed from the effective-range relations of Chew, Goldberger, Low, and Nambu,[23] and the S-wave phase shifts were taken to obey the relation

$$2\,\delta_1 + \delta_3 = 0.229\,q,$$

which is suggested by Orear's analysis.[24] The results of this computation are shown by the solid line in Figs. 9 and 10.

In order to determine how sensitive the theory is to the choice of these small phase shifts, Uretsky then made three changes. First, he set δ_{11} to zero. The results here were incompatible with the experimental data presented, because the cross section became very large at the backward angles. Secondly he set δ_{31} and δ_{13} equal to zero, leaving the other parameters unchanged. The results of this computation are shown by the dotted lines in Figs. 9 and 10. Lastly, he used Anderson's values for the phase shifts δ_{11}, δ_{31} and δ_{13},[25] with the result shown by the "dash dot" curves in Figs. 9 and 10. Comparison of these predictions to the experimental points shows that the choice $\delta_{31} = \delta_{13} = 0$ yields the best fit to the data in both cases.

The results of Uretsky's calculations are surprisingly sensitive to the choice of these small phase shifts, which are not well known experimentally. However, the photoproduction data probably cannot be used at this time to determine the values of these small phase shifts. This inability arises in part from the large number of free parameters and in part from the errors in the theoretical expression due to the assumptions made in its derivation, which are estimated to be of the order of 10%. The verification of the theoretical differential cross section must therefore await more accurate determinations of the small pion-nucleon phase shifts.

ACKNOWLEDGMENTS

We would like to acknowledge the support and encouragement received from Professor A. Carl Helmholz. The theoretical discussions we had with Professor Geoffrey F. Chew, Dr. Jack Uretsky, and Dr. Michael Moravcsik were very helpful. The participation of Dr. William Imhof in the early phases of the work and the assistance of Mr. John Caris and Mr. Walton Perkins in taking the data is greatly appreciated. Finally we would like to thank Mr. Rudin Johnson and the synchrotron crew, and Mr. James Vale and the cyclotron crew for their help and cooperation during the experiments.

This work was done under the auspices of the U.S. Atomic Energy commission.

FOOTNOTES

1. J. Steinberger and S.A. Bishop, Phys. Rev. 86, 171 (1952).
2. White, Jacobson, and Schulz, Phys. Rev. 88, 836 (1952).
3. Jarmie, Repp, and White, Phys. Rev. 91, 1023 (1953).
4. G. Bernardini and E.L. Goldwasser, Phys. Rev. 94, 729 (1954).
5. Jenkins, Luckey, Palfrey, and Wilson, Phys. Rev. 96, 179 (1954).
6. Walker, Teasdale, Peterson, and Vette, Phys. Rev. 99, 210 (1955).
7. Tollestrup, Keck, and Worlock, Phys. Rev. 99, 210 (1955).
8. Beneventano, Bernardini, Carlson-Lee, Stoppini, and Tau. Nuovo cimento, 4, 323 (1956).
9. L.S. Osborne and B. Richter, in Proc. Ann. Rochester Conf. High Energy Nuclear Phys. 6, Sec I, 25 (1956).
10. Watson, Keck, Tollestrup, and Walker, Phys. Rev. 101, 1159 (1956).
11. G.F. Chew and F.E. Low, Phys. Rev. 101, 1597 (1956).
12. Chew, Goldberger, Low and Nambu, Phys. Rev. 106, 1345 (1957).
13. A. Lazarus, Stanford University private communication.
14. J.H. Malmberg and C.S. Robinson, Phys. Rev. 109, 158 (1958).
15. Imhof, Kalibjian, and Perez-Mendez, Rev. Sci. Instr. 29, 476 (1958).
16. Prof. P.R. Wilson, Cornell University private communcation.
17. R. Martin, Phys. Rev. 87, 1052 (1952).
18. J.H. Malmberg and L.J. Koester, Jr., "Tables of Nuclear Reaction Kinematics at Relativistic Energies," privately circulated tables, Physics Research Laboratory, University of Illinois, 1953.
19. M.J. Moravcsik, Phys. Rev. 104, 1451 (1956).
20. Taylor, Moravcsik, and Uretsky, to be published UCRL-8317.
21. Uretsky, Kenney, Knapp, and Perez-Mendez, Phys. Rev. Letters 1, 12 (1958).
22. A similar evaluation has been made by Prof. C.S. Robinson of the University of Illinois whose results are in agreement with ours.[21]
23. Chew, Goldberger, Low, and Nambu, Phys. Rev. 106, 1337 (1957).
24. J. Orear, Nuovo cimento 4, 856 (1957).
25. H.L. Anderson, Proc. Ann. Rochester Conf. High Energy Nuclear Phys. 6, Sec. I, 20, (1956).

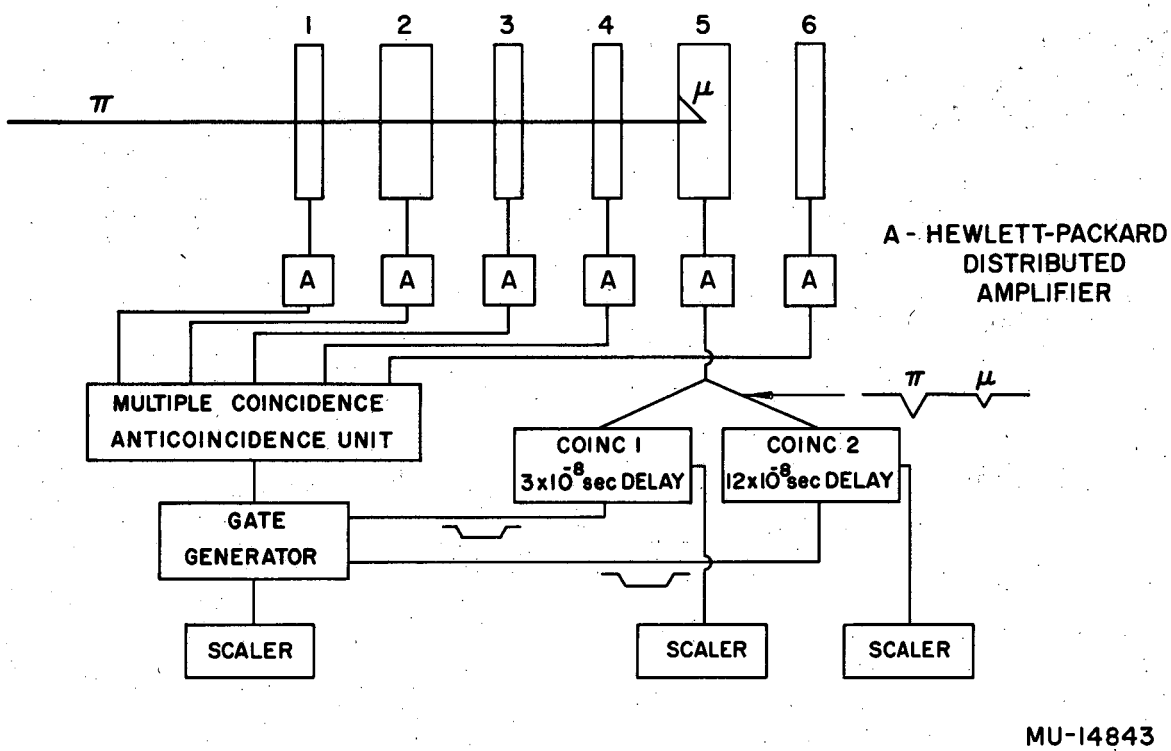

Fig. 1. Block diagram of π-μ electronics.

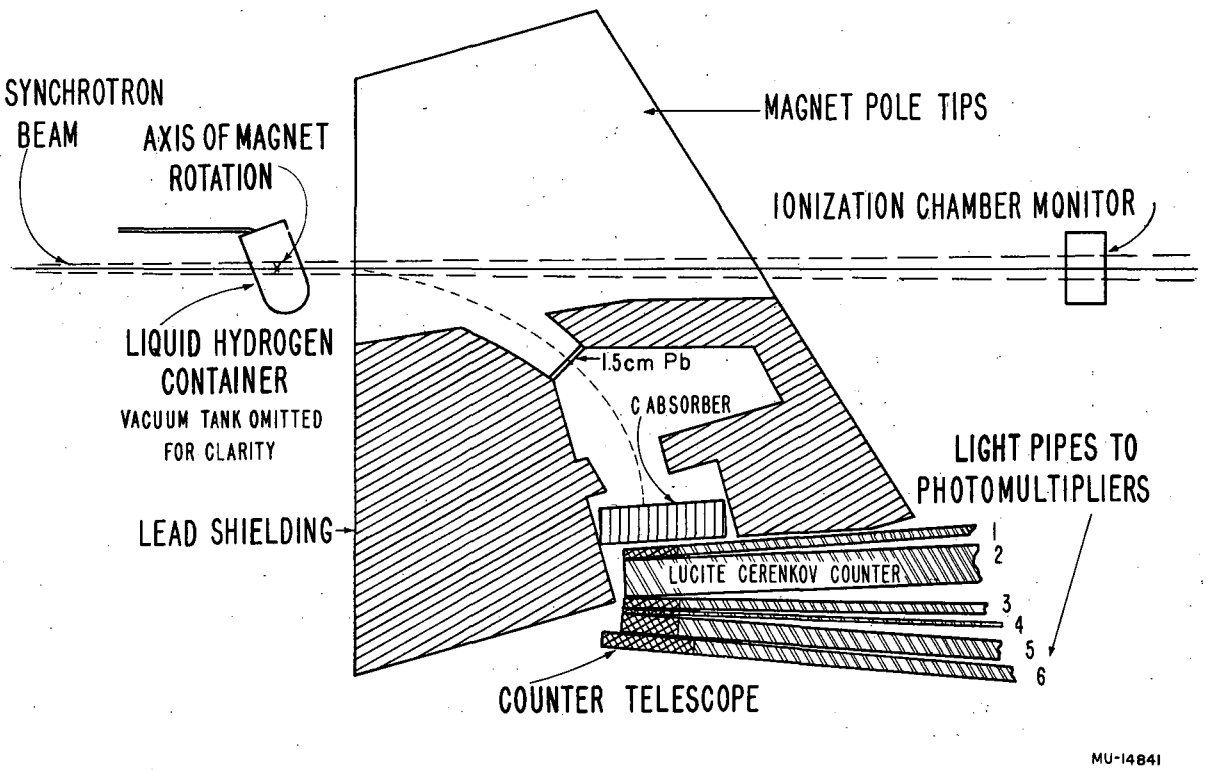

Fig. 2. Counter telescope used in the small-angle measurements.

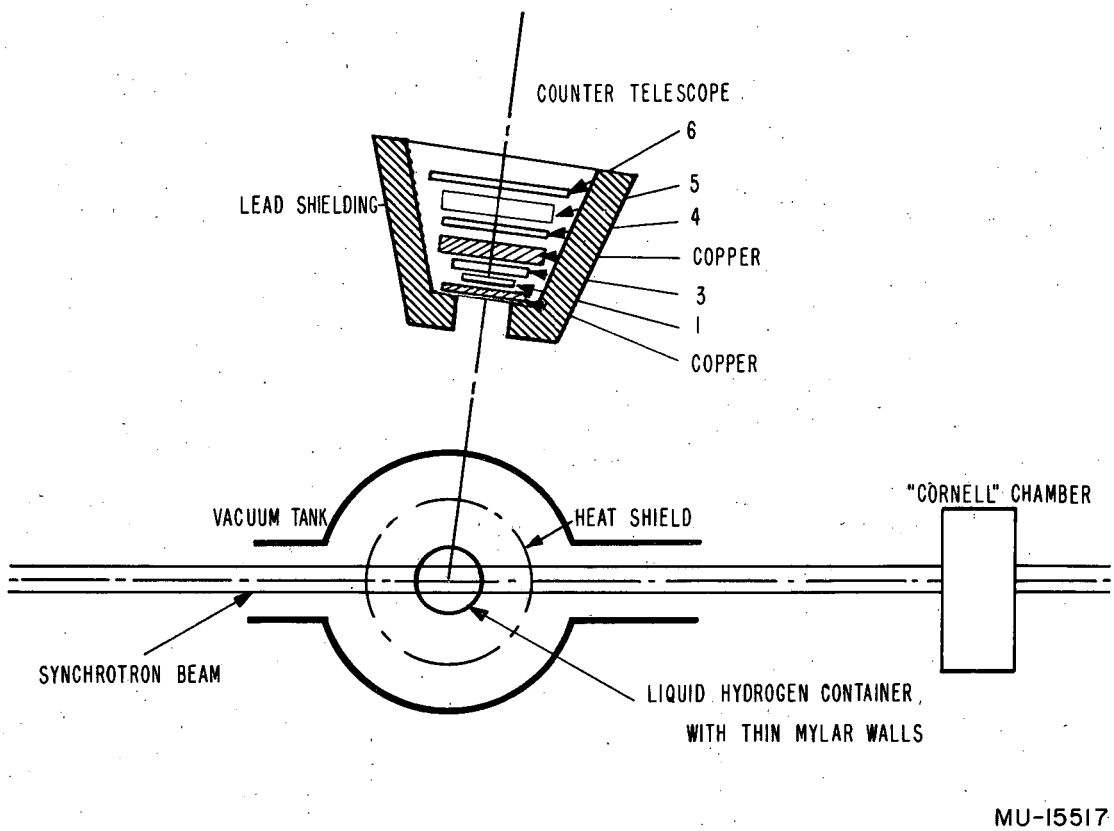

Fig. 3. Counter telescope used in the wide-angle measurements.

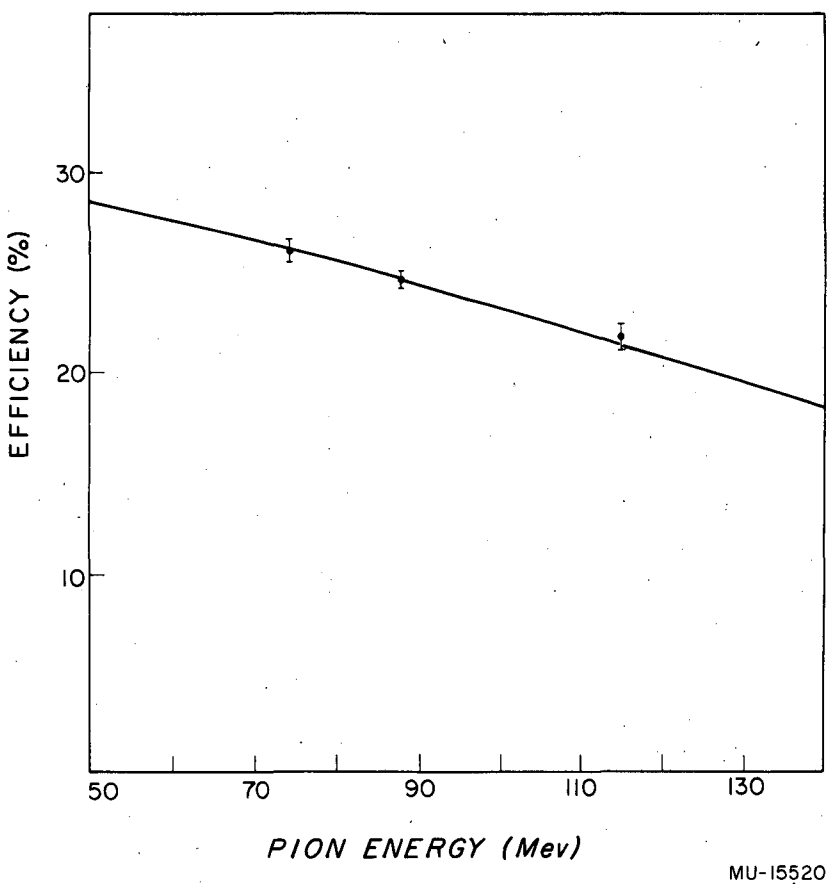

Fig. 4. Wide-angle telescope efficiency as a function of pion energy, from the cyclotron calibration. The solid surve represents the calibration utilizing the half-life curve and the measured absorption cross sections; the experimental points represent the ratio of pions incident to pions counted by means of π-μ decay.

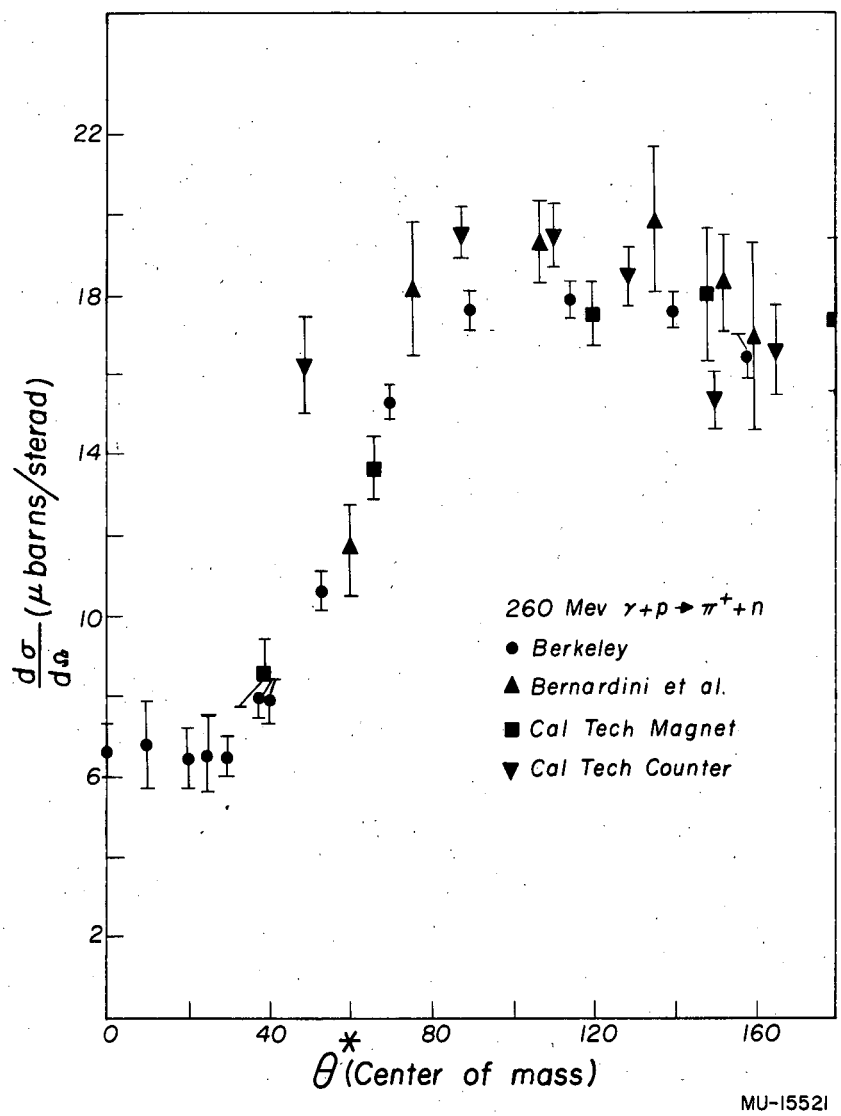

Fig. 5. The differential cross section for positive photopion production from hydrogen at a photon energy of 260 Mev. Superimposed on the data reported here are the results of the magnet and counter groups' determinations at the California Institute of Technology and the data taken from Bernardini's compilation.

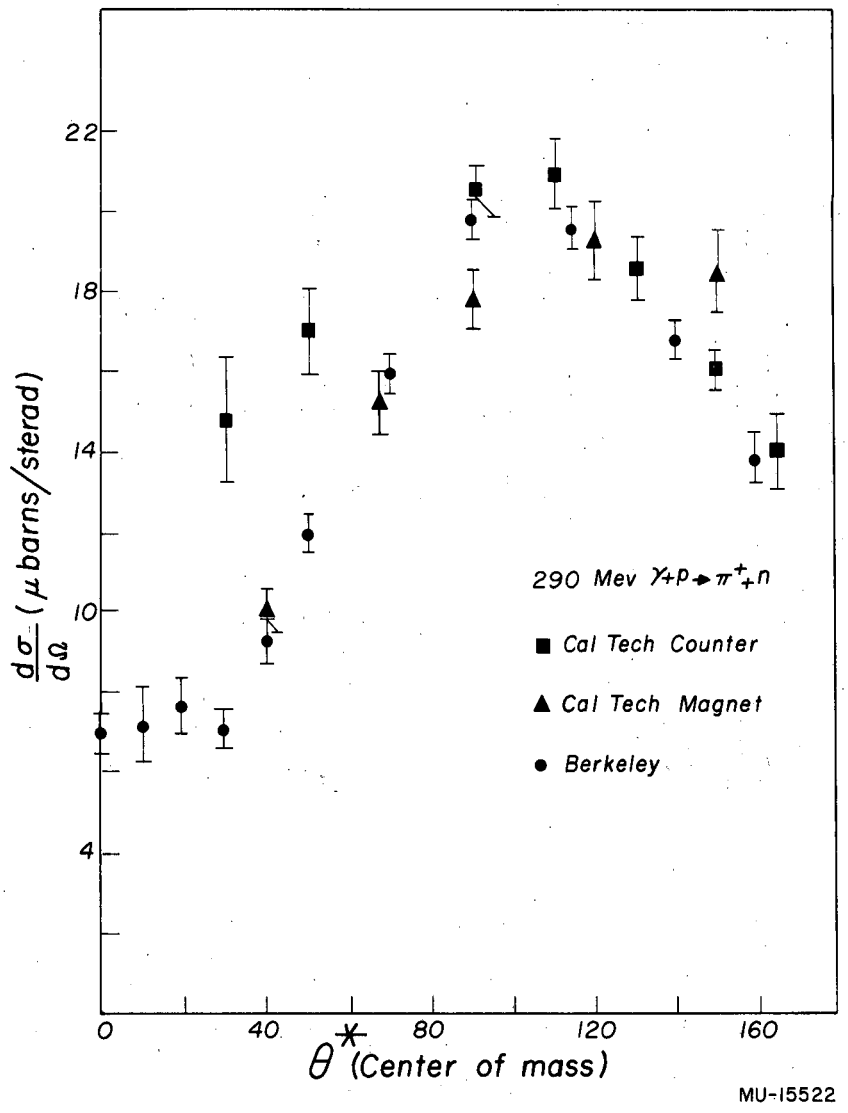

Fig. 6. The differential cross section for positive photopion production from hydrogen at a photon energy of 290 Mev. Superimposed on the data reported here are the results of the magnet and counter groups' determinations at the California Institute of Technology.

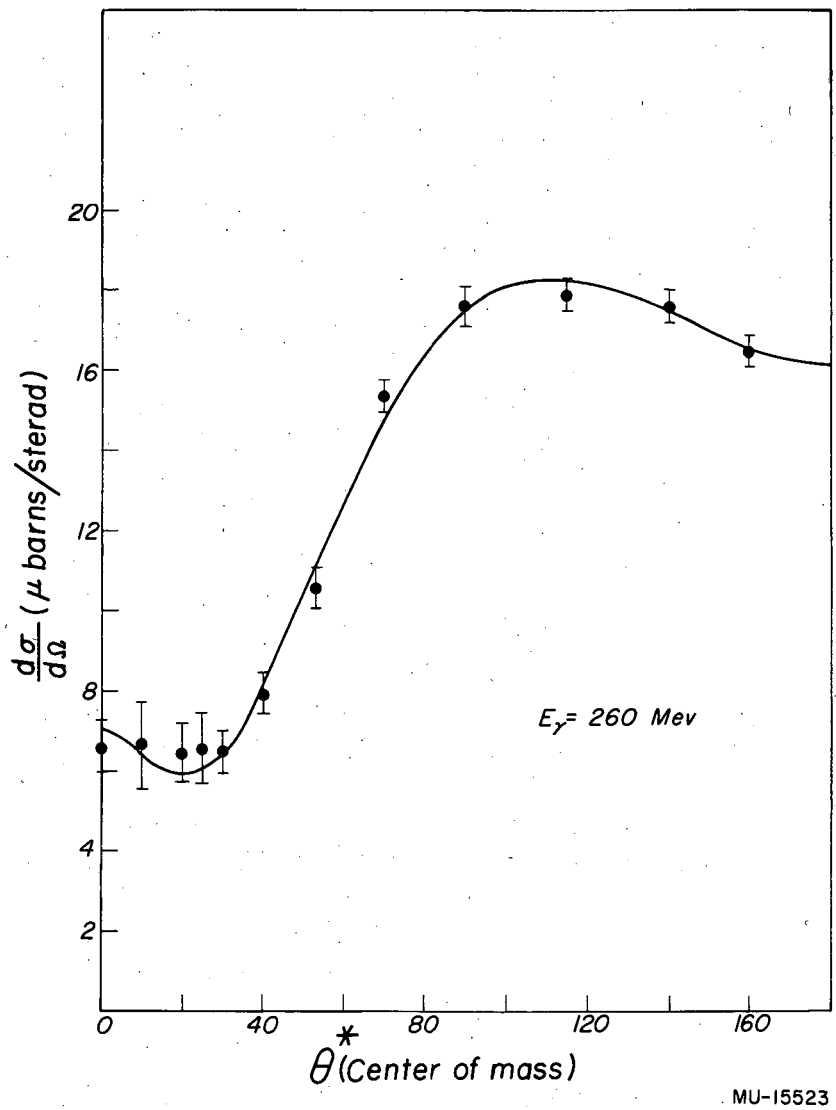

Fig. 7. Differential cross section for positive photopion production from hydrogen at 260 Mev. The solid curve represents the Moravcsik fit to the data.

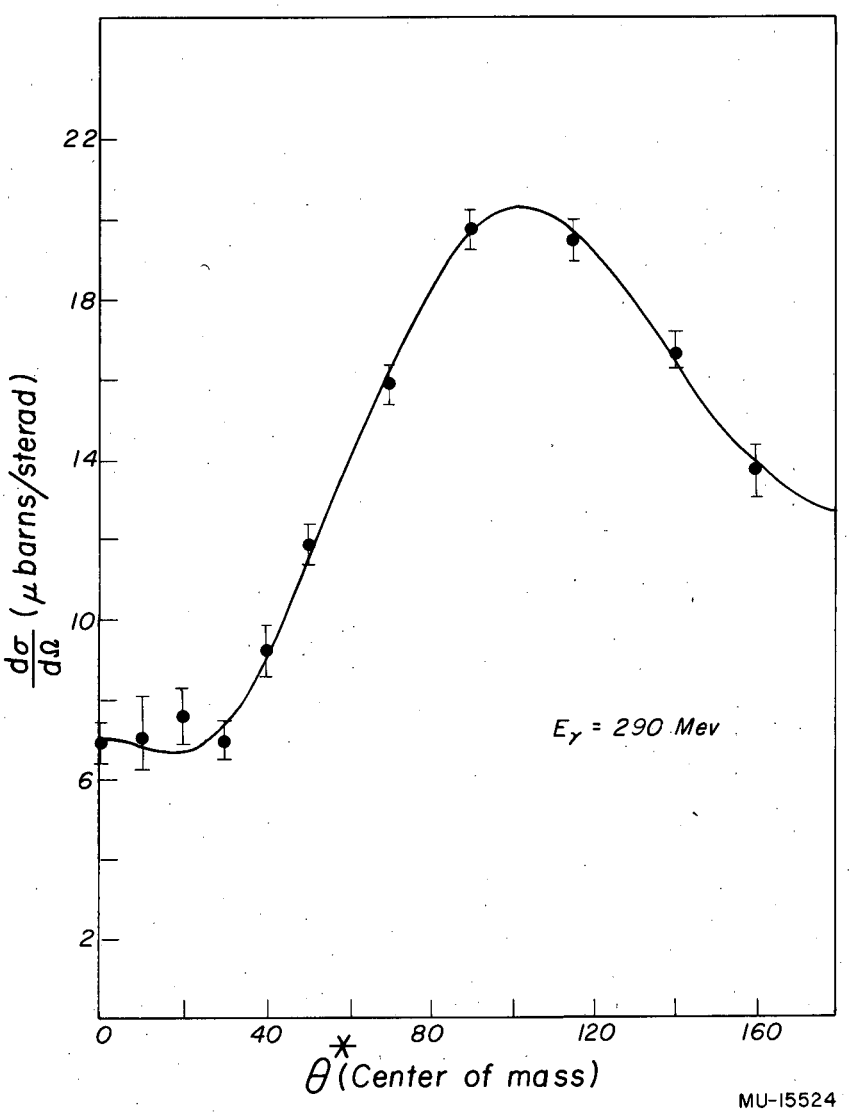

Fig. 8. Differential cross section for positive photopion production from hydrogen at 290 Mev. The solid curve represents the Moravcsik fit to the data.

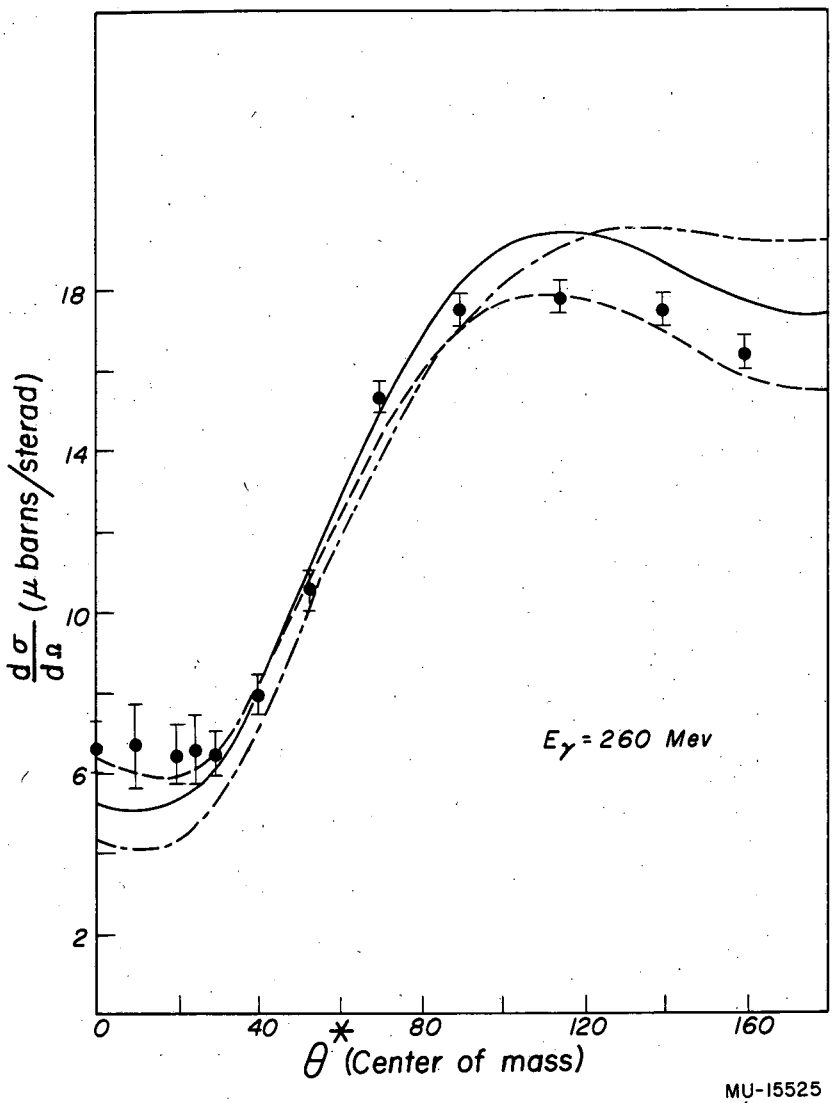

Fig. 9. Differential cross section for positive photopion-production from hydrogen at 290 Mev. For an explanation of the curves. see the text.

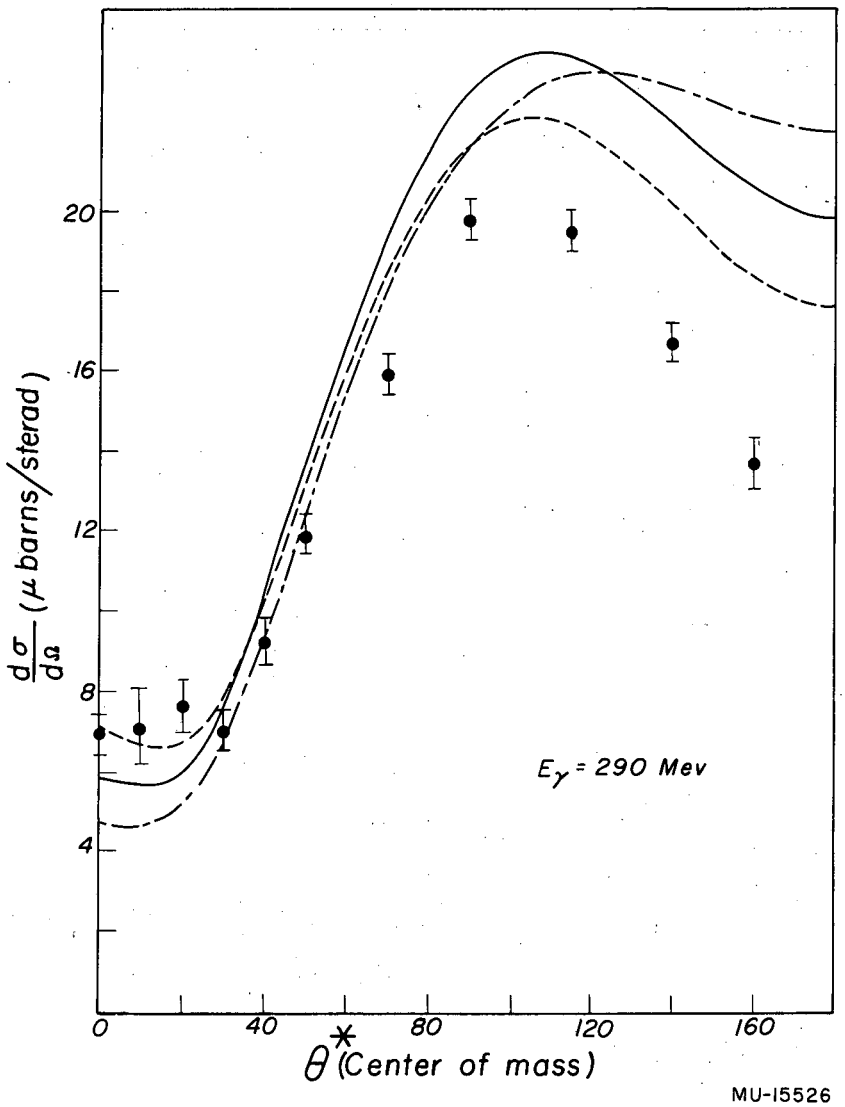

Fig. 10. Differential cross section for positive photopion production from hydrogen at 290 Mev. For an explanation of the curves, see the text.